Dynamics of Shear Alignment in a Lamellar Diblock Copolymer: Interplay of Frequency, Strain Amplitude, and Temperature

V. K. Gupta, R. Krishnamoorti, Z-R. Chen, and J. A. Kornfield*

Chemical Engineering 210-41, California Institute of Technology, Pasadena, California 91125

S. D. Smith, M. M. Satkowski, and J. T. Grothaus

Procter & Gamble, Cincinnati, Ohio 45239

Received June 29, 1995; Revised Manuscript Received November 7, 1995[⊗]

ABSTRACT: Rheo-optical methods are used to examine the combined effect of shear frequency, strain amplitude, and temperature on the direction and kinetics of flow-induced alignment in lamellar block copolymers. The development of shear-induced alignment in a nearly symmetric polystyrene−polyisoprene diblock (ODT ≃ 164 °C) is recorded in real time using flow birefringence as a probe of the transient lamellar orientation distribution. As alignment progresses during large amplitude oscillatory shearing, the birefringence shows an initial "fast" and a later "slow" change. While increasing strain amplitude (γ_o) generally speeds both the fast and the slow processes, below a critical γ_o the slow process is not observed and a well-aligned state is not achieved. The transient birefringence observed at a particular frequency and temperature, but different strain amplitudes, can be partially superposed by scaling time with $\gamma_o^{n(\omega)}$. However, the "fast" and "slow" processes require different values of $n(\omega)$. Estimates of $n(\omega)$ show that effects of strain are highly nonlinear and stronger than the simple rescaling of time in terms of either cumulative strain ($\sim t\gamma_o$) or cumulative flow energy ($\sim t\gamma_o^2$). The effect of temperature enters most strongly through the shift of time scale of molecular relaxations (a_T).

1. Introduction

External forces from flow, magnetic, or electric fields can be used to affect structural rearrangements in a wide range of complex fluids. Among these, block copolymers represent an important class of nanostructured materials. In spite of a considerable body of work on flow and electric field induced alignment in block copolymers,[1−18] understanding of the underlying processes is lacking. Until recently, investigations of flow alignment in lamellar diblocks centered on elucidating "parallel" alignment (layers aligned normal to the shear gradient direction). Following the discovery that large amplitude oscillatory shear at different frequencies could produce either parallel or "perpendicular" alignment (layers normal to the vorticity direction),[7,8] researchers have strived to gain insight into the mechanisms of both alignments and the selection of one over the other. Toward this end, experiment and theory have concentrated almost entirely on the effects of temperature and shear frequency. However, our recent discovery that strain amplitude can select between parallel and perpendicular orientations at a constant shear frequency and temperature[19,20] indicates that the nature of the alignment process is more complex.

To unravel the intricate dynamics during shear alignment, *in-situ* observations in real time are essential. Transient birefringence measurements provide an effective means to monitor the alignment process with high time resolution.[15,20] In an earlier paper,[20] we showed that alignment of a lamellar PS−PI block copolymer starts with a "fast" process that transforms the initial isotropic orientation distribution of the lamellar normals to an anisotropic distribution. For most shearing conditions this transformation of the orientation distribution occurs *via* a depletion that is predominantly along the flow direction (eliminating "transverse layers", *i.e.*, normal to the flow); however, at very high shear frequencies, the nature of the alignment process changes, and the perpendicular component of the orientation distribution disappears faster than the transverse component. This is surprising in light of existing notions regarding alignment: transverse layers are believed to be the least stable under shear[3] and, therefore, expected to disappear fastest. The initial, rapid process is followed by a later "slow" process, which eliminates all but one orientation along either the gradient direction (parallel) or the vorticity axis (perpendicular). We have also shown that in a frequency regime lying between the frequencies that induce parallel and perpendicular alignment, strain amplitude can control the direction of alignment.[19] Our results indicate a complex interplay of temperature, shearing frequency, and strain amplitude in controlling the changes in the orientation distribution during shearing.

In this paper, we focus on the role of strain amplitude and temperature in the evolution of microstructure during shear alignment. Following a brief description of the material and methods (section 2), we describe the effect of strain amplitude on the transient birefringence and shear alignment at different frequencies and temperatures (section 3). Then we discuss the alignment kinetics and implications of our collective results.

2. Experimental Section

We used a nearly symmetric polystyrene−polyisoprene diblock copolymer with $M_w \simeq 20$ kg/mol and $M_w/M_n \leq 1.06$. Rheological determination of the order−disorder transition temperature indicated $T_{ODT} \simeq 164$ °C.[21]

Rheo-Optical Characterization. Simultaneous, quantitative measurements of dynamic stress and birefringence were performed on a Rheometrics RSA II modified for rheo-optical measurements. Experimental details have been presented earlier.[23]

Light propagating along the velocity gradient direction (axis 2) probes the projection of the refractive index tensor in the

[⊗] Abstract published in *Advance ACS Abstracts,* January 1, 1996.

0024-9297/96/2229-0875$12.00/0

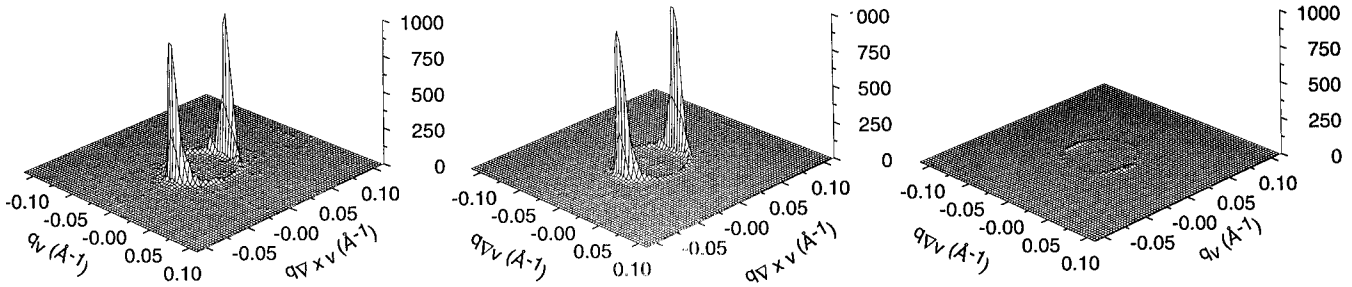

Figure 1. SAXS patterns observed in a PS−PI sample that was sheared at $\omega = 1$ rad/s, $T = 120$ °C, and $\gamma_0 = 95\%$ for 16 000 s.

plane formed by the flow direction (axis 1) and the vorticity axis (axis 3), *i.e.* $\Delta n_{13} = n_{11} - n_{33}$. For PS−PI diblocks, the birefringence is dominated by the form contribution resulting from the microphase-separated structure.[24,25] Therefore, the evolution of the steady offset in $\Delta n_{13}^{(d)}(t)$ probes the orientation distribution of the lamellae (Appendix A).

In the parallel orientation, the lamellae normal ($\hat{\mathbf{u}}$) points in the velocity gradient direction (axis 2) and is along the beam propagation direction. This results in zero birefringence in the 1,3-plane for a perfectly aligned parallel state. In contrast, perpendicular alignment ($\hat{\mathbf{u}} \parallel$ axis 3) corresponds to positive $\Delta n_{13}^{(d)}$ for PS−PI, since the form contribution has a higher index along the layers. The largest birefringence we have ever observed for a perpendicular aligned sample is $\Delta n_{max} \simeq 1 \times 10^{-3}$. For an orientation distribution biased along the transverse direction ($\hat{\mathbf{u}} \parallel$ axis 1) relative to the perpendicular direction, the 1,3-birefringence is also large but negative. While a final large, positive value of 1,3-birefringence unambiguously reflects predominant perpendicular alignment, many states can give a final near zero $\Delta n_{13}^{(d)}$. Therefore, final states with low $\Delta n_{13}^{(d)}$ are interpreted in combination with the changes in the small strain dynamic moduli (G', G'') to assign parallel alignment (Appendix A). The interpretation is confirmed by characterizing the final state of alignment using SAXS applied to separately prepared samples, as described below; the results are in accord with previous structural studies using TEM/SAXS for a very similar polymer system,[11] which establish that oscillatory shear produces aligned lamellae and correlate the direction of alignment with changes in G' and G''.

Shear alignment experiments have been performed using prolonged, large amplitude oscillatory shear. Before each alignment experiment, the sample is heated well into the disordered phase (180 °C) and is allowed to equilibrate for 15−20 min. It is then cooled to the desired temperature in the ordered state and equilibrated for 15 min. This procedure results in a reproducible initial condition, as confirmed by frequency sweep measurements using small strains. The rheo-optical results presented in this paper and in our earlier papers[19,20] are from the same sample, the experiments having been performed by simply cooling and reheating the polymer after loading it in the shearing cell. No evidence of any thermal or oxidative degradation, or cross-linking is observed in either the terminal behavior in the disordered state or the GPC traces for the polymer at the completion of the whole suite of experiments. Also no broadening or shifting of the T_{ODT} is observed over the whole suite of experiments.

Small Angle X-ray Scattering Measurements. A separate set of samples was prepared to characterize the final state of alignment using small-angle X-ray scattering (SAXS). Three samples were prepared. Each was heated above the ODT, cooled to the desired temperature, and characterized by small amplitude shearing to check $G^*(\omega)$ of the unaligned material. The samples were then subjected to selected shearing conditions that lie within the range explored in the rheo-optical experiments, then characterized again using small strain amplitude to record the final $G^*(\omega)$, and finally cooled to room temperature and carefully removed from the flow cell for further characterization. It is worth noting that the procedure of preparing samples for SAXS characterization is subject to complications that are not present in the suite of rheo-optical experiments.[27] Therefore, the primary significance of the SAXS results is to reveal the qualitative state of alignment that corresponds to the end of a representative birefringence trajectory.

X-ray scattering patterns were collected using a Siemens small angle scattering system, which includes an Anton Paar HR-PHK high-resolution pinhole optics system with a multiwire 2-D X-ray detector. The generator was a Rigaku RU-300 rotating anode operated at 40 kV and 40 mA with a 0.2 mm × 2 mm filament set in the spot focus mode. The X-ray beam is collimated by a 100 μm diameter pinhole placed approximately 490 mm from the focal spot. Another pinhole 300 μm in diameter is set 650 mm from the focal spot. This second pinhole reduces the parasitic scattering from the first pinhole. The sample to detector distance is approximately 650 mm. This arrangement leads to an incident X-ray spot on the sample of a diameter about 0.2 mm. Samples are set on a micrometer holder that is adjusted to place the sample such that the incident beam strikes the sample completely. All samples where in the range 0.6−0.8 mm in thickness. X-ray patterns were collected for either 10 or 30 min. The patterns were normalized for differences in thickness and collection time. Background scattering was negligible (less than 1% of the signal in the peaks). In fact, background scattering amounted to less than 1 or 2 counts per pixel per 30 min except very near the beam stop. Therefore, background corrections were ignored in these first qualitative runs.

3. Results

The viscoelastic spectrum for the present PS−PI material in the disordered state and the ordered, but initially unaligned, state is reported in Gupta *et al.*[20] The critical frequency (ω_c') associated with a crossover in the relaxation dynamics from being dominated by the macromolecular response to being dominated by the microstructural response is estimated to be $\omega_c' \approx 3-7$ rad/s at 120 °C. At shear frequencies above ω_c' (*e.g.*, $\omega \geq 10$ rad/s at 120 °C for $\gamma_o > 0.4$) parallel alignment is achieved, and at lower frequencies perpendicular alignment is induced (*e.g.*, $\omega = 1$ rad/s at 120 °C for $\gamma_o > 0.3$).[20]

Here we examine the effects of strain and temperature on flow alignment. The dynamics of perpendicular and parallel alignment are very sensitive to the amplitude of the oscillatory strain, as described in sections 3A and 3B, respectively. The effect of temperature on the evolution of alignment during shear shows that qualitatively similar alignment is observed at similar reduced frequencies and that the predominant alignment at temperatures close to T_{ODT} is along the perpendicular direction for this sample (section 3C).

A. Effect of Strain on the Development of Perpendicular Alignment. As in our earlier paper, perpendicular alignment was induced by shearing at $\omega = 1$ rad/s and $T = 120$ °C. The small angle X-ray scattering observed from a sample aligned with $\gamma_o =$

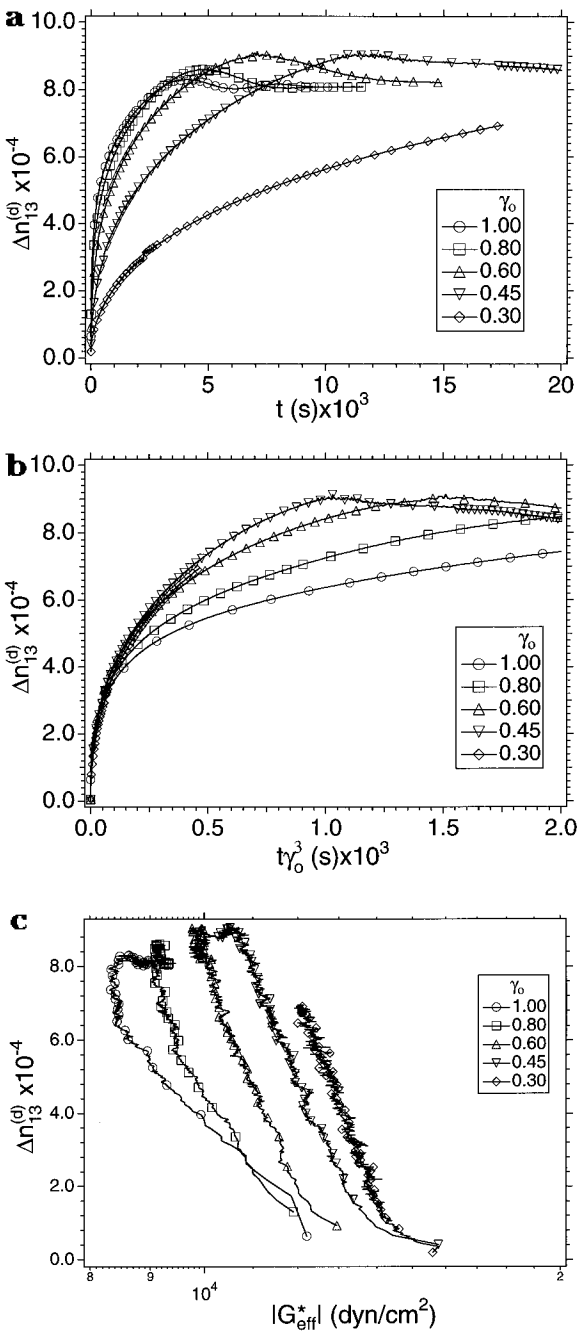

Figure 2. (a) Transient 1,3-birefringence observed during shearing at $T = 120$ °C, $\omega = 1$ rad/s, and different strain amplitudes. (b) Evolution of $\Delta n_{13}^{(d)}(t)$ plotted against scaled time. (c) Transient birefringence plotted against the effective modulus ($|G^*_{eff}(t)|$) measured during alignment. Sparsely spaced markers have been used in plots a−c to distinguish between the curves.

0.95 confirmed this assignment of the final orientation (Figure 1). The patterns obtained with the X-ray beam along either the velocity or the velocity gradient directions showed strong anisotropy parallel to the vorticity direction, while the scattering was very weak and nearly isotropic when the X-ray beam was along the vorticity direction. Thus, SAXS patterns indicated that lamellae normals lie predominantly along axis 3.

To investigate the effect of strain amplitude on the perpendicular alignment process, shearing experiments were performed at a constant frequency and temperature of $\omega = 1$ rad/s and $T = 120$ °C, and with strain amplitudes from 0.3 to 1 (Figure 2a). On the basis of the transient birefringence observed at $\gamma_o = 0.3$, lower strain amplitudes were not attempted, since the alignment process became prohibitively slow. The transient birefringence during shear possessed similar shapes at the different strain amplitudes, indicating similar trajectories for the evolution of the orientation distribution. However, the time scale of the alignment process was significantly reduced with increasing strain amplitude. Shearing at $\gamma_o \geq 0.45$ ultimately resulted in a high value of $\Delta n_{13}^{(d)}$ ($\simeq 8.2 \times 10^{-4}$, within 10% of the plateau $\Delta n_{13}^{(d)}$ for the sample prepared for SAXS, Figure 1), indicating that the lamellar layers were oriented along the perpendicular direction.

By inspection of the shape of $\Delta n_{13}^{(d)}(t)$, it is clearly not possible to superpose the complete transient birefringence at different strain amplitudes by any simple rescaling of time. To qualitatively describe the nonlinear effect of γ_o and contrast its effect on fast *vs* slow processes, we seek rescalings $t/\tau(\gamma_o)$ that superpose the early or late portions of $\Delta n_{13}^{(d)}(t)$. Due to the absence of any predictions for the form of $\tau(\gamma_o)$, we attempted to collapse the curves using $\tau(\gamma_o) \sim \gamma_o^n$, restricting n to integers. With this scaling, the initial transient birefringence up to $\approx 3 \times 10^{-4}$ is superposed when plotted against $\gamma_o^3 t$ (Figure 2b). This scaling indicates an effect of γ_o stronger than can be attributed simply to either cumulative strain ($\gamma_o t$) or work ($\gamma_o^2 t$) during shearing at a particular frequency ω. The latter part of the transient birefringence is not superposed by this scaling, since the effect of strain during this period of the evolution of alignment is weaker than during the initial rise. In turn, this may signal a change in the mechanism of alignment from the "fast" process to the "slow" one.

As described in our earlier paper,[20] at all strain amplitudes the effective dynamic modulus (G^*_{eff}) during shear alignment showed an initial rapid drop whose magnitude increases with γ_o. Subsequent decreases occurred much more gradually. Here, we examine the relation between the orientation distribution (as inferred from the transient birefringence) and the modulus by plotting $\Delta n_{13}^{(d)}(t)$ against $|G^*_{eff}(t)|$ (Figure 2c). The evolution of $|G^*_{eff}(t)|$ as a function of microstructure (to the extent it is indicated by $\Delta n_{13}^{(d)}(t)$) changes with strain. The shifts in $|G^*_{eff}(t)|$ *vs* $\Delta n_{13}^{(d)}(t)$ toward lower modulus with increasing strain may reflect either strain softening of a given microstructure corresponding to a particular $\Delta n_{13}^{(d)}$ or differences in the microstructure corresponding to a given $\Delta n_{13}^{(d)}$ along the distinct trajectories.

B. Effect of Strain on the Development of Parallel Alignment. We have previously shown that prolonged large amplitude ($\gamma_o \geq 0.5$) shear at $\omega = 10-100$ rad/s at 120 °C led to similar aligned states, though *via* different trajectories.[20] Rheo-optical characterization had suggested that the final alignment was in the parallel direction. This conclusion is supported by the measurements of small angle X-ray scattering from samples subjected to a similar shearing history (Figure 3). Intense scattering peaks along the velocity gradient direction were observed in the patterns obtained with the X-ray beam along the vorticity or the velocity directions. Weak and nearly isotropic scattering was evident when the sample was viewed along the velocity gradient direction.

It was shown earlier[20] that during alignment at 10 rad/s, the initial process was dominated by a rapid

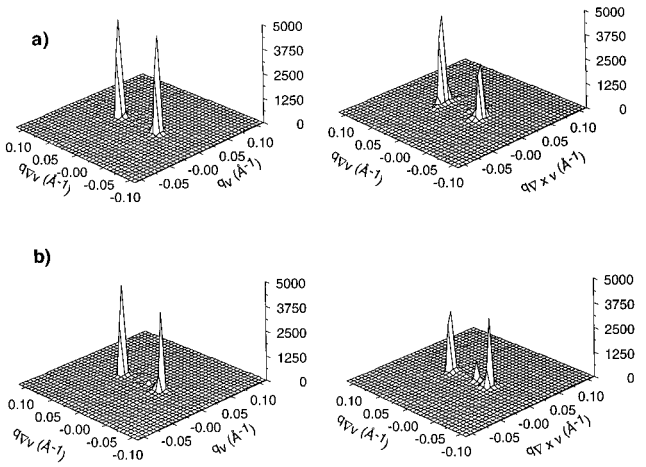

Figure 3. SAXS patterns observed in PS−PI samples that were sheared at (a) $\omega = 10$ rad/s, $T = 120$ °C, and $\gamma_o = 100\%$ for 16 000 s, and (b) $\omega = 100$ rad/s, $T = 120$ °C, and $\gamma_o = 50\%$ for 16 000 s. On the same vertical scale, the intensity of scattering with the X-ray beam along the velocity gradient direction is effectively zero (maximum peak count <50).

depletion of the projection of the orientation distribution along the transverse direction ($\hat{\mathbf{u}}$ || axis 1) relative to the perpendicular direction ($\hat{\mathbf{u}}$ || axis 3), manifested as a rapid increase in $\Delta n_{13}^{(d)}(t)$. Conversely, at 100 rad/s, during the initial fast process, the projection of the orientation distribution along the perpendicular direction decreased *faster* than that along the transverse direction, indicated by the sharp decrease of birefringence toward a large negative value. At intermediate frequencies (20 rad/s $\leq \omega \leq$ 60 rad/s), both projections decreased at comparable rates, with the birefringence remaining small throughout the alignment process.[20]

To understand the role of strain during parallel alignment, we performed experiments over a range of strain amplitudes at three frequencies: 10, 30, and 100 rad/s at 120 °C.

***ω* = 10 rad/s at 120 °C.** Shearing with strain amplitudes from 0.5 to 1.0 resulted in qualitatively similar transient birefringence during shear (Figure 4a) and final aligned states with almost identical small-strain dynamic moduli. During the initial fast process, $\Delta n_{13}^{(d)}(t)$ increased rapidly to a value $\sim 3 \times 10^{-4}$ for $\gamma_o \geq 0.5$. Refinement of alignment during the slow process was accompanied by a gradual decrease in the birefringence to a near zero value.[20]

Shearing with $\gamma_o < 0.5$ produced qualitatively different results (Figure 4a). The transient birefringence during the fast process at $\gamma_o = 0.4$ increased to $\sim 3 \times 10^{-4}$, like at higher strain amplitudes; however, no slow refinement of the alignment was evident and $\Delta n_{13}^{(d)}(t)$ remained at this approximate value for over 9000 s. Thus, unlike the larger strain amplitudes, for $\gamma_o = 0.4$, the final state was not highly aligned.[28] The birefringence during shearing at $\gamma_o = 0.3$, was even more unexpected. Here, $\Delta n_{13}^{(d)}(t)$ increased throughout the duration of shearing and exceeded $\sim 1/3\ \Delta n_{max}$ ($\sim 3 \times 10^{-4}$) (Figure 4a). This effect of strain amplitude was qualitatively similar to our earlier observations[19,20] during shearing at 4 rad/s and $T = 120$ °C, where moving from high strain amplitude ($\gamma_o = 1.1$) to low ($\gamma_o = 0.4$) changed the direction of shear-induced alignment from parallel to perpendicular. The small strain moduli after shearing at $\omega = 10$ rad/s with $\gamma_o = 0.3$ and 0.4 were between those of the initially unaligned state and those observed after alignment at higher strain amplitudes.

Successive shearing at $\gamma_o = 0.8$ was performed after cessation of prolonged (~7000 s) shearing at $\gamma_o = 0.3$ (Figure 4b). This resulted in a sharp decrease of $\Delta n_{13}^{(d)}(t)$ toward zero, in a manner reminiscent of the "flipping" of perpendicular alignment to parallel observed by Kornfield *et al.*[16] The small-strain dynamic moduli measured at the end of this shearing process were identical to those obtained for a well-aligned parallel state. The time scale for approaching parallel alignment was similar to that observed when shearing at $\gamma_o = 0.8$ starting from an unaligned initial state (*cf.*, Figure 4a).

The rate of both the fast and slow processes increased with an increase in strain (Figure 4a). Once again, simple rescaling of time did not yield a single master curve for all the different strain amplitude experiments. However, the initial rise in $\Delta n_{13}^{(d)}(t)$ could be nearly superposed for $\gamma_o \geq 0.4$ using a scaled time $\gamma_o^5 t$ (Figure 4c). In contrast to the cubic scaling (*i.e.* $\gamma_o^3 t$) obtained in the perpendicular alignment case, here the effects of strain amplitude on the fast process were even more highly nonlinear. Again, such a strong effect of strain amplitude cannot be attributed simply to either cumulative strain ($\gamma_o t$) or work ($\gamma_o^2 t$) done during shear. The failure to superpose the transient birefringence observed upon shearing at $\gamma_o = 0.3$ suggested that the nature of the alignment mechanism changed as γ_o decreased.

The slow refinement of alignment could be partially superposed by rescaling time, using $\gamma_o^3 t$ for $\gamma_o > 0.55$ (Figure 4d). At lower strain amplitudes there were systematic deviations from this scaling, indicating stronger-than-cubic dependence on γ_o for $\gamma_o \leq 0.55$. Thus, while strain amplitude affected both the fast and slow processes strongly, the effects of strain on the rate of each process were distinct and suggested distinct underlying processes.

In contrast to results at $\omega = 1$ rad/s, the transient birefringence during shearing at 10 rad/s exhibited a strong connection with the effective dynamic modulus ($|G^*_{eff}|$) (Figure 4e). Across a large range of strain amplitudes, intermediate states having similar orientation distributions (to the extent this is indicated by equal $\Delta n_{13}^{(d)}(t)$ values along the alignment trajectory) have similar moduli (Figure 4e). This correlation suggests that the effective modulus at $\omega = 10$ rad/s, $T = 120$ °C, and $\gamma_o = 0.4-1.0$ is largely determined by the orientation distribution of the lamellae.

***ω* = 30 rad/s at 120 °C.** For the strain amplitudes probed, *i.e.* from 0.5 to 0.7, a small value of $\Delta n_{13}^{(d)}(t)$ was observed throughout the alignment process (Figure 5). The small strain dynamic moduli measured after shearing were identical to those obtained after shear at 10 rad/s. Therefore, the final state is inferred to be aligned in the parallel orientation. The small value of birefringence throughout the process could be interpreted in terms of a continual decrease in the projections of the orientation distribution along the perpendicular and the transverse directions at comparable rates and a continual increase in the projection along the parallel direction (S_{11}, $S_{33} \rightarrow \sim 0$ and $S_{22} \rightarrow \sim 1$; see Appendix). Furthermore, in this case, the transient birefringence at different strain amplitudes was quite distinct, and rescaling time could not superpose any part of the different curves.

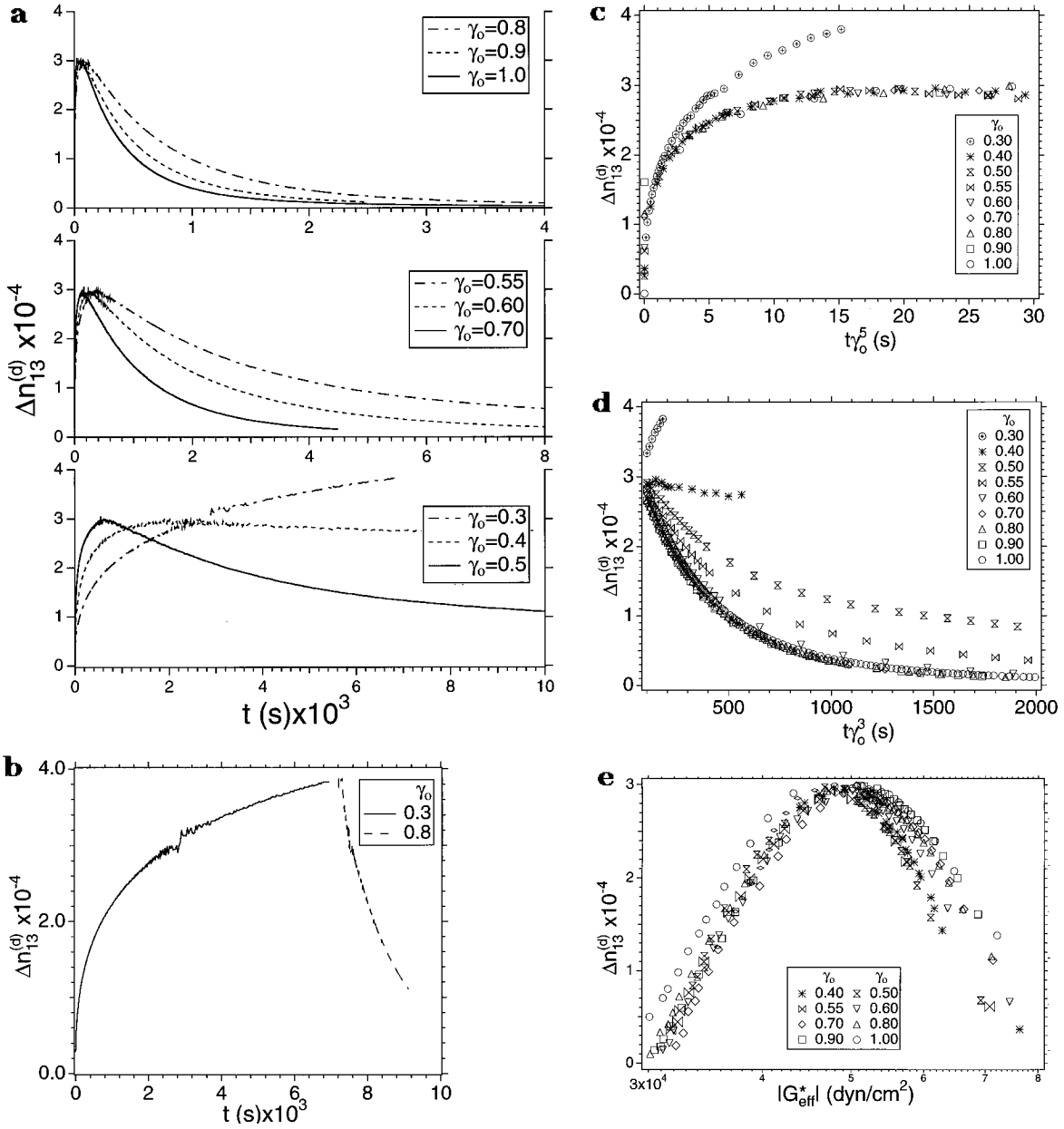

Figure 4. (a) Transient 1,3-birefringence observed during shearing at $T = 120$ °C, $\omega = 10$ rad/s and different strain amplitudes. (b) Evolution trajectory for $\Delta n_{13}^{(d)}(t)$ during shearing ($T = 120$ °C, $\omega = 10$ rad/s), first with a strain amplitude of 0.3 followed by a strain amplitude of 0.8. (c) Evolution of $\Delta n_{13}^{(d)}(t)$ during the initial fast process plotted against scaled time. (d) Evolution of $\Delta n_{13}^{(d)}(t)$ during the slow process plotted against scaled time. (e) Transient birefringence plotted against the effective modulus ($|G^*_{\text{eff}}(t)|$) measured during alignment at different strain amplitudes. Sparsely spaced markers have been used to distinguish between the curves.

$\omega = 100$ rad/s at 120 °C. As we reported earlier,[20] the birefringence observed during shearing at 100 rad/s was negative, indicating an orientation distribution with an enhanced projection of *transverse* orientation relative to the perpendicular (Figure 6a). We believe that the parallel alignment is also enhanced. Biaxial orientation enriched in the transverse and parallel alignments was recently reported by Okamoto *et al.*[29] working with polystyrene−poly(ethylene-*alt*-propylene) diblock melts and by Pinheiro *et al.*[30] using blends of PS−PI with polystyrene. Since our first report of this surprising trajectory, *i.e.* rapid disappearance of the perpendicular projection relative to the transverse projection *en route* to parallel alignment,[20] similar observations have been reported by Zhang and Wiesner using SAXS.[31]

Analogous to shearing at 10 rad/s, the rate of alignment at 100 rad/s increased with strain (Figure 6a). Shearing at sufficiently large $\gamma_o \geq 0.3$ produced parallel alignment *via* distinctive fast and slow processes. At 100 rad/s, strain amplitude had a much larger effect on the extremum value of $\Delta n_{13}^{(d)}(t)$ than it did at 10 rad/s. At relatively low strain amplitudes ($\gamma_o = 0.2$), $|\Delta n_{13}^{(d)}(t)|$ increased throughout the shearing process, as in the case of shearing at 10 rad/s using $\gamma_o = 0.3$.

Because the minimum value of $\Delta n_{13}^{(d)}(t)$ was not constant across the different strain amplitudes, rescaling time in terms of strain cannot fully describe the strain dependence. However, to provide a comparison with the results at lower ω, we obtained rough estimates: the fast process showed an approximate time scaling as the cubic power (γ_o^3) while the slow process exhibited a scaling of approximately γ_o^4. These estimates show that here the slow process is more sensitive

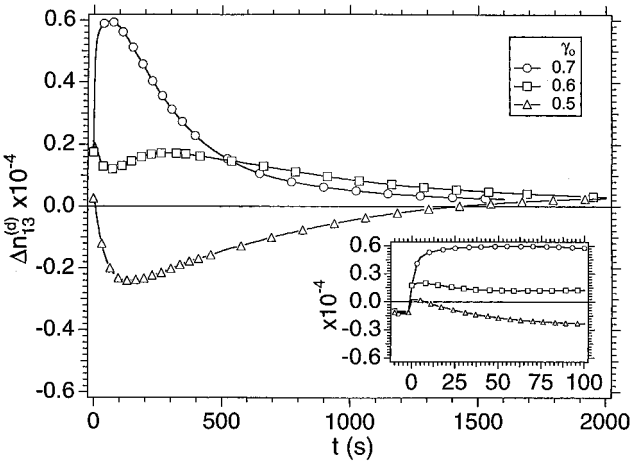

Figure 5. Transient 1,3-birefringence observed during shearing at T = 120 °C, ω = 30 rad/s, and different strain amplitudes. Sparsely spaced markers have been used to distinguish between the curves.

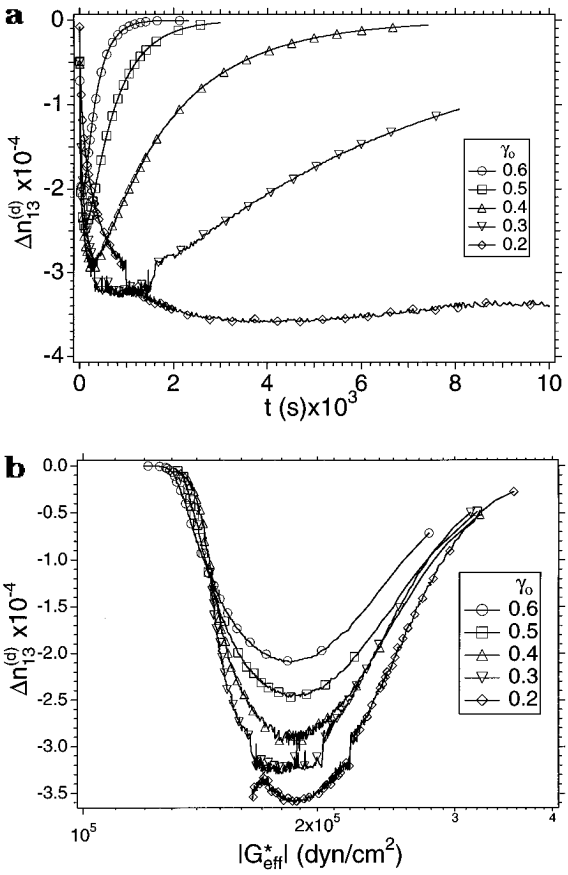

Figure 6. (a) Transient 1,3-birefringence ($\Delta n_{13}^{(d)}(t)$) observed during shearing at T = 120 °C, ω = 100 rad/s, and different strain amplitudes. (b) Transient birefringence plotted against the effective modulus ($|G^*_{\text{eff}}(t)|$) measured during alignment. Sparsely spaced markers have been used to distinguish between the curves.

to γ_o than the fast process—unlike the trend at 1 and 10 rad/s.

A relationship between $\Delta n_{13}^{(d)}(t)$ and $|G^*_{\text{eff}}(t)|$ is again evident (Figure 6b). The family of curves of $\Delta n_{13}^{(d)}(t)$ *vs* $|G^*_{\text{eff}}(t)|$ have similar shapes, and the effective modulus corresponding to the minima in $\Delta n_{13}^{(d)}(t)$ is nearly constant ($|G^*_{\text{eff}}| \sim 1.9 \times 10^5$ dyn/cm^2) for the different strain amplitudes (Figure 6b).

C. Effect of Temperature. In an ordered block copolymer, dynamic and thermodynamic changes with temperature are expected to affect the evolution of shear-induced alignment, including the dependence of alignment on shear frequency and strain amplitude. We explore these effects by performing shear alignment experiments at temperatures lying above the T_g of the PS-rich microphase and below the T_{ODT}.

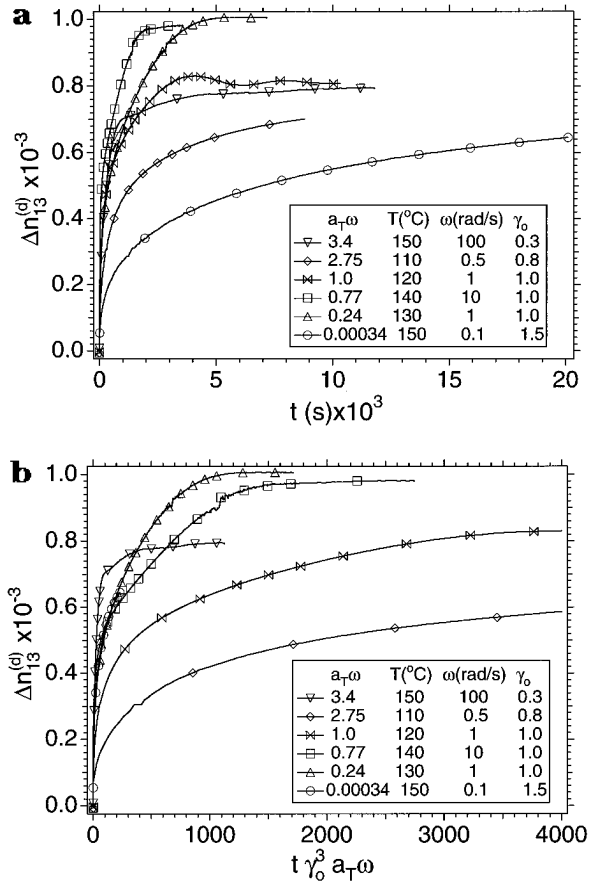

Figure 7. (a) Transient birefringence observed during perpendicular alignment at various reduced frequencies. (b) Transient birefringence plotted as a function of scaled time. Sparsely spaced markers have been used to distinguish between the curves.

Increasing temperature led to a wider range of accessible conditions that produced alignment. At 100 °C, experimental limitations restricted the strain amplitude to $\gamma_o < 0.3$ and the birefringence saturated at intermediate negative values and was neither indicative of parallel alignment (*i.e.* near zero) nor indicative of perpendicular alignment.[32,33] Rather, this negative $\Delta n_{13}^{(d)}(t)$ at 100 °C suggested an orientation distribution with a modestly larger projection of lamellae normals along the transverse direction than along the perpendicular direction. Similar results for the transient birefringence were observed at a higher temperature of 110 °C (for $a_T\omega \approx 11$ and 55 rad/s). Therefore, we could not unambiguously assign an alignment direction for a number of the shearing experiments at 100 and 110 °C. The only exception was at $a_T\omega \approx 2.75$ rad/s and 110 °C, where shearing produced a large and positive birefringence ($\sim 7 \times 10^{-4}$), indicating significant perpendicular alignment (Figure 7a). At temperatures of 120 °C or higher it was possible to use larger strain amplitudes, which induced alignment within a few hours. With increasing temperature, the accessible frequency range shifted to lower $a_T\omega$ and fewer shearing conditions induced parallel alignment. Beyond 130 °C we were able to achieve only perpendicular alignment.

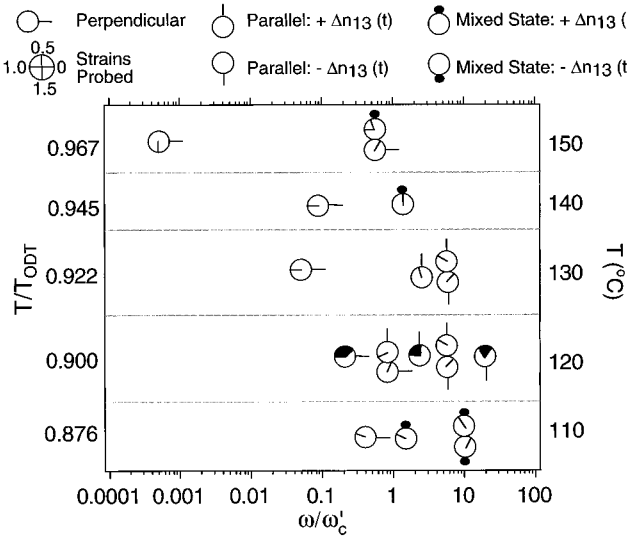

Figure 8. Summary of alignment results from shearing at different sets of temperature, frequency, and strain amplitude. The final state of alignment (or partial alignment) is indicated on the outside of each circular marker. The strain amplitude used are marked within the circular marker; a filled region indicates a range of γ_o was probed. Two circles atop each other indicate different alignment results at the same temperature and frequency, but with different strain amplitudes. Results at $T < 110$ °C are not shown as we did not observe definitive alignment. The approximate value of $\omega_c' = 5$ rad/s ($T_0 = 120$ °C) is used to normalize the shear frequency.

As perpendicular alignment can be produced at all temperatures ranging from 110 to 150 °C, it is possible to explore the interplay of temperature with shear frequency and strain amplitude by comparing the evolution of $\Delta n_{13}^{(d)}(t)$ at different temperatures, *en route* to perpendicular alignment (Figure 7a). Increasing temperature from 110 to 140 °C produces a faster and larger rise in $\Delta n_{13}^{(d)}(t)$ (Figure 7a). However, it is necessary to account for the effects of γ_o, ω, and T in order to compare the various trajectories. Therefore, we plot $\Delta n_{13}^{(d)}$ as a function of scaled time $t\gamma_o^3 a_T \omega$, where the effect of strain amplitude is accounted for by using γ_o^3, which is appropriate for the fast process *en route* to perpendicular alignment. While not completely capturing the dependency of the alignment process on temperature, frequency, and strain, such a scaling is effective in partially superposing the transient birefringence, especially for the fast process at $a_T\omega = 0.77$, 0.24, and 0.000 34 rad/s (Figure 7b, *cf.* Figure 2c). Furthermore, with respect to this scaled time, as $a_T\omega$ decreases, we observe faster evolution of $\Delta n_{13}^{(d)}$ for all frequencies except $a_T\omega = 3.4$ at 150 °C[34] (Figure 7b).

As in other studies[7,11,12,17] we find that the change in chain dynamics with temperature is indeed a major factor in determining the ultimate alignment direction. When viewed as a function of reduced frequency, a particular value of $a_T\omega$ (close to $a_T\omega_c'$) demarcates two regimes for PS−PI: low frequencies inducing perpendicular orientation and higher frequencies leading to parallel orientation (Figure 8). For parallel alignment in PS−PI, an additional regime at very low reduced frequencies, *i.e.* at temperatures close to T_{ODT}, has been found recently by Zhang *et al.* (at $T/T_{ODT} \simeq 0.973$ and $\omega/\omega_c' \simeq 0.0257$).[18] However, we are unable to obtain parallel alignment in our PS−PI material at such high temperatures (close to T_{ODT}) and low frequencies ($\omega/\omega_c' \simeq 0.0007$) (see Figure 8). Patel *et al.*[17] have also found only perpendicular alignment at the lowest reduced frequencies they probe ($T/T_{ODT} \simeq 0.984$ and $\omega/\omega_c' \simeq 0.000\,02$).

The two-dimensional plot in terms of T/T_{ODT} *vs* ω/ω_c' used by other researchers[7,17] is effective in capturing the different regimes of alignment. However, it is necessary to represent the third dimension associated with strain amplitude and capture the interplay of γ_o with ω and T in controlling the direction and dynamics of alignment (Figure 8). We discover two distinct crossover regions where strain amplitude plays an important role: (a) between perpendicular and parallel alignment, where the *direction* of alignment depends on the strain amplitude, and (b) between the frequencies leading to parallel alignment but *via* either a positive or a negative transient $\Delta n_{13}^{(d)}(t)$, where changes in strain amplitude affect the sign and shape of the transient $\Delta n_{13}^{(d)}(t)$.

4. Discussion

A. Implications of the Current Results. Toward the goal of predicting the direction, degree, and dynamics of flow-induced alignment, various authors have suggested mechanisms that might explain distinct orientations (*e.g.*, selective melting leading to perpendicular alignment).[7,18] Other investigators have suggested the possibility that two or more mechanisms may act in combination to produce alignment.[6,11]

Indeed, our results indicate that during the course of shearing there is a transition in the character of alignment, as though one process overtakes another in importance. This is clearly manifested in the time scale of the development of alignment—an early ("fast") and a late ("slow") change is evident in the transient birefringence for each alignment trajectory. More than one process appears to underlie these distinct transformations. This is indicated by the distinct strain dependencies of the time scales for the fast and slow processes, with the dependency varying with frequency. For example at 10 rad/s and 120 °C, the time scale varies roughly as γ_o^{-5} for the fast process *vs* γ_o^{-3} for the slow process (Figure 4c,d). In contrast, at 1 rad/s and 120 °C, the time scale of the fast process scales as γ_o^{-3} while the slow process shows a weaker strain dependence.

Multiplicity of processes is also suggested by the distinct ways that shearing transforms the orientation distribution. For example, upon varying $a_T\omega$ (*i.e.*, frequency and temperature) the trajectory of alignment can involve

- a rapid disappearance of the projection along the transverse direction with an increase either along the parallel direction or along the perpendicular direction, or
- a rapid disappearance of the projection of the orientation distribution along the perpendicular direction—sometimes faster than that along the transverse direction—*en route* to parallel alignment.

The changes in the relative stability of transverse and perpendicular projections with ω and γ_o suggest a competition between two processes: one that predominantly eliminates the transverse projection and another that eliminates the perpendicular component. The latter appears to dominate the fast process at all γ_o for $\omega = 100$ rad/s and 120 °C (note the negative $\Delta n_{13}^{(d)}$ trajectory in Figure 6a). The recent SAXS results of Zhang and Wiesner are in accord with alignment trajectories that pass through large, negative $\Delta n_{13}^{(d)}$ and

with the notion that distinct processes dominate the fast and slow stages of alignment.[31] However, their interpretation of the evolution of alignment emphasizes the role of entanglement, even though negative birefringence trajectories have been previously reported on the present system,[20] which is at most marginally entangled. On moving from 100 to 10 rad/s, the perpendicular component becomes relatively stable compared to the transverse (trajectory changes sign from negative to positive $\Delta n_{13}^{(d)}$, *cf.* Figures 6a and 4a). The results of Zhang and Wiesner are not in accord with parallel alignment trajectories for which $\Delta n_{13}^{(d)} > 0$ throughout the process.

A competition between distinct processes is also suggested by the interplay of ω and γ_o observed at "intermediate" frequencies. One example is in the crossover region between the two qualitatively different routes to parallel alignment: at a particular frequency (*e.g.* 30 or 100 rad/s), the relative persistence of the transverse component increases with decreasing γ_o (the minimum in $\Delta n_{13}^{(d)}$ becomes more negative as γ_o decreases, Figures 5 and 6a). Another example is in the crossover region between the shearing conditions inducing parallel and perpendicular alignment. At 4 rad/s and T = 120 °C, strain has the dramatic effect of *selecting the direction* of flow-induced alignment.[19] Thus, while the mechanisms that lead to parallel and perpendicular alignment may both be occurring at this ω and T, the one that leads to parallel alignment becomes dominant as strain increases.

This interplay of strain amplitude and shear frequency in determining the evolution of alignment also has important implications on the different pictures put forward by previous researchers to explain selection of the route and direction of alignment in block copolymers. It has been argued that flow energy ($\sim\sigma\gamma_o$) could overcome the microphase-separation energy and disrupt the lamellar microdomains; if followed by a re-formation along a preferred direction, this disruption would lead to alignment.[5,6,11] The choice of a preferred direction (parallel or perpendicular alignment) is believed to depend critically on the shear rate.[7,11,13] However, the whole suite of results outlined in this paper and in our previous work[20] indicates that alignment is not simply controlled by either the shear rate, the cumulative strain, or the flow energy. For instance at 120 °C,

a) shearing conditions of [ω = 10 rad/s, γ_o = 1] and [ω = 30 rad/s, γ_o = 0.5] are not widely separated in terms of *shear rate* ($\sim\omega\gamma_o$) but show drastically different transient birefringence (Figures 4a and 5) and correspondingly distinct microstructural changes;

b) $\Delta n_{13}^{(d)}(t)$ observed during shearing at a particular frequency (*e.g.*, 1, 10, or 100 rad/s) but different strain amplitudes (γ_o) cannot be superposed using *cumulative strain* ($\sim\gamma_o t$);

c) *flow energy* ($\sim|G^*_{eff}|\gamma_o^2\omega$) during shearing at [30 rad/s, γ_o = 0.7] is similar to that during shearing at [100 rad/s, γ_o = 0.3], but the trajectories during alignment at these two conditions are dramatically different (birefringence in Figures 5 and 6a).

Another recent study proposes that in PS−PI, the ultimate alignment direction at a particular shear rate and temperature is chosen to correspond with the minimum modulus (G^*).[17] However, we have shown in our earlier paper that the alignment direction does not correlate with minimization of either the modulus during shear (G^*_{eff}) or the small strain modulus $G^*(\omega)$ after alignment.[20]

B. Parameters Controlling Flow-Induced Alignment. It is widely accepted that the molecular and microstructural dynamics that cause alignment upon shearing are a function of the combined effects of molecular composition, temperature (T), and shear frequency (ω).[3−10,14,15]

Among the several influences of temperature is the change of the time scale for conformational relaxation of the polymeric constituents of the block copolymer. Typically, this is accounted for by lumping the temperature effect into a single shift factor a_T, a procedure that does not capture the different time−temperature shifts for the different microphases. Temperature also couples with the molecular composition (*via* χN) to alter the degree of segregation, with weaker segregation as $T \rightarrow T_{ODT}$. Consequently, higher temperatures reduce the viscoelastic contrast between the microphases in PS−PI and also increase the magnitude of fluctuations. While the role of viscoelastic contrast has been acknowledged as a factor,[15,17,18] it remains uninvestigated. Influence of strength of fluctuations has been characterized by Koppi *et al.*[7] using T/T_{ODT} as a characteristic parameter.

Shear frequency is regarded as the other key factor during shear, and it is believed that shearing in different dynamical regions leads to either perpendicular or parallel alignment.[7,15,17,18] Koppi *et al.*[7] have suggested three regimes: the "domain" or "defect" controlled regime at very low frequencies where the response on the scale of whole grains or domains (or defect dynamics) dominates; the "microstructural" regime at frequencies where the distortion of the microphase-separated structure dominates; and the "polymeric" regime at high frequencies where the distortion of macromolecules dominates viscoelasticity (demarcated from the "microstructural" regime by ω_c'). Thus, mapping alignment conditions[7] with respect to T/T_{ODT} and ω/ω_c' offers some insight into the role of both frequency and temperature and provide common grounds for comparison between different studies. Indeed, for both PEP−PEE[7,15] and PS−PI,[11,12,17,18,20] perpendicular alignment is observed in a frequency regime with $\omega/\omega_c' < 1$. However, while PEP−PEE shows parallel alignment in a regime with $\omega/\omega_c' \ll 1$, in PS−PI several studies[11,12,17,18,20] find parallel alignment only for $\omega/\omega_c' > 1$, with one report[18] citing parallel alignment for $\omega/\omega_c' \ll 1$. In PEP−PEE, no alignment has been reported in a regime with $\omega/\omega_c' > 1$.

While shear frequency and temperature play important roles, they are by no means the only parameters that influence macroscopic alignment. Other flow parameters (*e.g.*, strain amplitude) and material characteristics (*e.g.*, viscoelastic contrast) may also be important. At fixed ω and T, strain amplitude influences the stress response, the shear rate, and the magnitude of distortion. Therefore, γ_o can be expected to have significant consequences as well. Surprisingly, it has received little attention previously and only few results exist.[6,11,35] Winey *et al.*[11] have reported that for PS−PI melts, strain amplitudes lower than 0.01 do not induce alignment while $\gamma_o \simeq 0.01-0.05$ are effective in producing alignment. Morrison *et al.*[6] investigated SBS triblocks under steady shear and observed improved alignment with an increase in the cumulative strain imposed. However, no systematic study of strain amplitude has been undertaken and scant attention has been paid in theoretical modeling to the effects of strain amplitude.[3,4,9,10,14] Our study forms the first body of

results that establish the importance of strain as a controlling parameter that is intricately linked with shear frequency and temperature in determining the dynamics of alignment.

The available theoretical literature on alignment also lacks treatment of the complex dynamics resulting from an orientation distribution within a polydomain material. Current theories focus almost exclusively on the properties of microstructures that are uniformly aligned, with an emphasis on elucidating the relative stability of monodomains in different orientations, when subjected to an applied field.[3,4,9,10,14,36] However, as the orientation distribution has to evolve dynamically from that of a polydomain material to a well-aligned material, consideration of the stability of the ultimate microstructure alone is not sufficient. Indeed, our results indicate that the dynamics of alignment from an unaligned state to distinct aligned states involve a rich cascade of processes whose relative importance and rates vary nonlinearly with γ_o, ω, and T.

The variety of trajectories of alignment challenge us to understand the kinematics of the polydomain material during shear. A fundamental grasp of such issues would elucidate the physics underlying the reorientation of the grains and the process of ultimate alignment of the lamellae along a preferred direction. We believe that considerable opportunity exists in modeling and simulation of these effects, which in turn could yield valuable insights to guide the unified design of materials and processing conditions to exploit flow-induced alignment.

5. Summary

The effect of reduced frequency on flow-induced alignment in PS−PI is essentially to demarcate two regimes:[17] at low ωa_T, *i.e.* near T_{ODT}, the predominant alignment is perpendicular, and at higher $a_T\omega$, *i.e.* generally at lower T, parallel alignment is observed. Strain amplitude has highly nonlinear effects on the rate of alignment induced by large-amplitude oscillatory shear, which cannot be explained simply in terms of either the cumulative strain or the work done during shear. At all temperatures and shear frequencies, there appears to be a critical strain amplitude, below which a well-aligned state is not attainable. The effect of γ_o extends even to controlling the direction of alignment induced by shearing.

The trajectories of alignment indicate that during shear, complex dynamics underlie the transformation of the distribution of lamellar orientations in an unaligned state to a well-aligned parallel or perpendicular orientation. Consequently, is not sufficient to model the system from the perspective of a monodomain or uniformly oriented microdomain. During shear at a constant frequency, the nature of the alignment process evolves as the orientation distribution changes and is manifested in distinct fast and slow processes in the transient birefringence. There is also a change in the character of the alignment process as a function of the frequency of the applied shear. These changes suggest that multiple mechanisms might be at work during flow-induced alignment, even *en route* to a given orientation. Both strain amplitude *and* shear frequency determine the dominant mechanism at a given temperature.

Acknowledgment. This research was carried out with the support of the NSF-PYI (J.A.K.), Chevron, and Raychem. We would like to thank Dr. Steven Paulin for helpful discussions.

Appendix A

For PS−PI, the form contribution to the birefringence ($\Delta\mathbf{n}_f$) resulting from the block copolymer microstructure is estimated to be at least 3 times the intrinsic or "molecular" contribution ($\Delta\mathbf{n}_i$).[24,25] Consequently, the observed birefringence can be approximately related to the second moment of the orientation distribution of the lamellae:

$$\Delta n = -n_0(\mathbf{S} - \mathbf{I})$$

where $\Delta\mathbf{n}$ is the deviatoric part of the refractive index tensor and $\mathbf{S}$ is the order parameter tensor. $S_{ij} = \langle u_i u_j \rangle$, with $\mathbf{u}$ being the normal to the lamellae and $\langle ... \rangle$ denoting an average over the orientation distribution. $\mathbf{I}$ is the identity tensor, and n_0 is a constant of proportionality that depends on the strength of segregation and the resulting periodic variation of the mean refractive index. Empirically, n_0 can be determined from birefringence measurements in samples in which the orientation distribution is known. We estimate the value of n_0 for the present sample by the largest birefringence we have ever observed for a perpendicularly aligned sample, $\Delta n_{max} \simeq 1 \times 10^{-3}$.

Complete characterization of $(\mathbf{S} - \mathbf{I})$ requires the value of n_0 and measurement of at least two projections of the refractive index tensor. In the present experiments, we are limited to observing just one projection.[26] Therefore, we can provide bounds on the orientation distribution and make reasonable inferences about the trajectory of orientation. Ongoing TEM and SAXS measurements on samples removed at intermediate states of alignment will provide the basis for more definitive interpretation.

Large 1,3-birefringence values provide relatively unambiguous results. In particular, $n_{11} - n_{33} = n_0$ uniquely corresponds to an order parameter tensor with $S_{33} = 1$ as its only non-zero component, *i.e.*, perfect perpendicular alignment. Similarly, $n_{11} - n_{33} = -n_0$ can only mean $\mathbf{S}$ has $S_{11} = 1$ as its only non-zero component, *i.e.*, perfect "transverse" alignment. The interpretation becomes more ambiguous as the birefringence decreases. Observing zero birefringence in the 1,3-plane can correspond to any uniaxial distribution that is symmetric about axis 2, *e.g.*, the initial isotropic state or the parallel aligned state.[20]

Therefore, in our experiments, to interpret a small birefringence, we take into account the dynamic modulus, the SAXS results, and the context within an overall trajectory.

References and Notes

(1) Keller, A.; Pedemonte, E.; Willmouth, F. M. *Colloid Polym. Sci.* **1970**, *238*, 25. Folkes, M. J.; Keller, A.; Scalisi, F. P. *Colloid Polym. Sci.* **1973**, *251*, 1.

(2) Bates, F. S.; Fredrickson, G. H. *Annu. Rev. Phys. Chem.* **1990**, *41*, 525. Bates, F. S. *Science* **1991**, *251*, 898. Safinya, C. R.; Sirota, E. B.; Bruinsma, R. F.; Jeppesen, C.; Plano, R. J.; Wenzel, L. J. *Science* **1993**, *261*, 588. Idziak, S. H. J.; Safinya, C. R.; Hill, R. S.; Kraiser, K. E.; Ruths, M.; Warriner, H. E.; Steinberg, S.; Liang, K. S.; Israelachvili, J. N. *Science* **1994**, *264*, 1915.

(3) Cates, M. E.; Milner, S. T. *Phys. Rev. Lett.* **1989**, *62*, 1856. Bruinsma, R.; Rabin, Y. *Phys. Rev. A* **1992**, *45*, 994. Goulian, M.; Milner, S. T. *Phys. Rev. Lett.* **1995**, *74*, 1775.

(4) Fredrickson, G. H. *J. Rheol.* **1994**, *38*, 1045. Girovich, E. *Macromolecules* **1994**, *27*, 7063. Girovich, E. *Macromolecules* **1994**, *27*, 7339. Girovich, E. *Phys. Rev. Lett.* **1995**, *74*, 482.

(5) Hadziioannou, G.; Mathis, A.; Skoulious, A. *Colloid Polym. Sci.* **1979**, *257*, 136.

(6) Morrison, F. A.; Winter, H. H. *Macromolecules* **1989**, *22*, 3533. Morrison, F. A.; Winter, H. H.; Gronski, W.; Barnes, J. D. *Macromolecules* **1990**, *23*, 4200.
(7) Koppi, K.; Tirrell, M.; Bates, F. S.; Almdal, K.; Colby, R. H. *J. Phys. II* **1992**, *2*, 1941.
(8) Koppi, K.; Tirrell, M.; Bates, F. S. *Phys. Rev. Lett.* **1993**, *70*, 1449.
(9) Amundson, K.; Helfand, E.; Davis, D. D.; Quan, X.; Patel, S. S.; Smith, S. D. *Macromolecules* **1991**, *24*, 6546. Amundson, K.; Helfand, E.; Quan, X.; Smith, S. D. *Macromolecules* **1993**, *26*, 2698.
(10) Amundson, K.; Helfand, E. *Macromolecules* **1993**, *26*, 1324.
(11) Winey, K. I.; Patel, S. S.; Larson, R. G.; Watanabe, H. *Macromolecules* **1993**, *26*, 2542.
(12) Winey, K. I.; Patel, S. S.; Larson, R. G.; Watanabe, H. *Macromolecules* **1993**, *26*, 4373.
(13) Larson, R. G.; Winey, K. I.; Patel, S. S.; Watanabe, H. *Rheol. Acta* **1993**, *32*, 245.
(14) Amundson, K.; Helfand, E.; Quan, X.; Hudson, S. D.; Smith, S. D. *Macromolecules* **1994**, *27*, 6559.
(15) Kannan, R. M.; Kornfield, J. A. *Macromolecules* **1994**, *27*, 1177.
(16) Kornfield, J. A.; Kannan, R. M.; Smith, S. D. *ACS Polym. Mater. Sci. Eng. Preprint* **1994**, *71*, 250.
(17) Patel, S. S.; Larson, R. G.; Winey, K. I.; Watanabe, H. *Macromolecules* **1995**, *28*, 4313.
(18) Zhang, Y.; Wiesner, U.; Spiess, H. W. *Macromolecules* **1995**, *28*, 778.
(19) Gupta, V. K.; Krishnamoorti, R.; Kornfield, J. A.; Smith, S. D. *Macromolecules*, Note to appear in Feb 12 issue.
(20) Gupta, V. K.; Krishnamoorti, R.; Kornfield, J. A.; Smith, S. D. *Macromolecules* **1995**, *28*, 4464.
(21) We performed a temperature sweep at a rate of 1 °C/min. At each temperature the dynamic moduli were measured using oscillatory shear at 10 rad/s and 2% strain. At T_{ODT}, both moduli (G', G'') exhibited a steep decrease, which was more pronounced for G'. Similar determination revealed a typical hysteresis behavior upon cooling with the transition temperature a few degrees lower than that during heating. The order−disorder transition temperature is also manifested in optical measurements as a steep decrease in the "apparent birefringence".[22] For yet unknown reasons, we observed T_{ODT} of 171 and 164 °C for two different batches for the same polymer sample. All the experiments reported in this paper were performed with the latter.
(22) In the microphase-separated state for block copolymers a small apparent birefringence results from depolarization of the polarized light upon transmission through a collection of randomly oriented lamellar grains.
(23) Kannan, R. M.; Kornfield, J. A. *Rheol. Acta* **1992**, *31*, 535. Kannan, R. M.; Kornfield, J. A.; Schwenk, N.; Boeffel, C. *Macromolecules* **1993**, *26*, 2050.
(24) Lodge, T. P.; Fredrickson, G. H. *Macromolecules* **1992**, *25*, 5643.
(25) Allan, P.; Arridge, R. G. C.; Ehtaiatkar, F.; Folkes, M. J. *J. Phys. D: Appl. Phys.* **1991**, *24*, 1381.
(26) For reasonable flow geometries, the 1,2-projection results in a retardation over too many orders due to the large path length (∼15 mm in our experiments).
(27) The procedure of preparing samples for SAXS is subject to variations in the samples and in the temperature controller, uncertainties in the precise sample geometry from sample to sample, possible distortion of the aligned structure during cooling and unloading, and, for the SAXS experiments performed with the beam along either the flow or vorticity directions, effects of cutting the sample.
(28) Quantitative characterization of the degrees of alignment is an important issue. It has been reported that strain amplitudes as low as 0.05 yield parallel alignment.[11] However, our transient birefringence results from shearing at 120 °C with strain amplitudes of 0.3 (ω = 10 rad/s) and 0.2 (ω = 100 rad/s) show that while the lamellar distribution has an enhanced projection along the parallel direction, the degree of alignment is *not* high (Figures 4a and 6a).
(29) Okamoto, S.; Saijo, K.; Hashimoto, T. *Macromolecules* **1994**, *27*, 5547.
(30) Pinheiro, B. S.; Winey, K. I. *Polym. Prepr. (Am. Chem. Soc., Div. Poly. Chem.)* **1995**, *36*, 174.
(31) Zhang, Y.; Wiesner, U. *J. Chem. Phys.* **1995**, *103*, 4784.
(32) At the lower temperatures (*i.e.*, 100 °C) prolonged shearing over several hours was possible only using moderate strain amplitudes ($\gamma_o \leq 0.3$). Higher strain amplitudes were not used due to limitations of our force transducer and flow cell geometry, and due to the possibility of melt fracture.
(33) Previous studies of shear alignment in PS−PI[11−13] have reported parallel alignment at low temperatures (near the T_g of the polystyrene-rich microphase) even using strain amplitudes as low as 0.05.
(34) The exclusion of $a_T\omega$ = 3.4 (*i.e.* 150 °C and 100 rad/s) from the trend may be because at this reduced frequency shearing at higher strains ($\gamma_o \sim 1.0$ as opposed to 0.3) results in $\Delta n_{13}^{(d)}(t)$ typical of parallel alignment. Though, $\Delta n_{13}^{(d)}(t)$ did not decrease completely to zero and resulted in a mixed state of alignment. Thus, this condition is reminiscent of 4 rad/s and 120 °C, where strain amplitude plays a dominant role with low γ_o (∼0.4) inducing perpendicular alignment and $\gamma_o \sim 1.1$ leading to parallel alignment.[19]
(35) Balsara, N.; Hammouda, B.; Kesani, P. K.; Jonnalagadda, S. V.; Straty, G. C. *Macromolecules* **1994**, *27*, 2566. Balsara, N. P.; Hammouda, B. *Phys. Rev. Lett.* **1994**, *72*, 360.
(36) Hudson, S. D.; Amundson, K. R.; Jeon, H. G.; Smith, S. D. *MRS Bull.* **1995**, *20*, 42.

MA950925C